An optimal adaptive quantization index modulation watermarking algorithm

Shaomin Zhu (朱少敏)[1*] and Jianming Liu (刘建明)[2]

[1]China Electric Power Research Institute, Beijing 100192, China

[2]State Grid Information and Telecommunication Co., Ltd., Beijing 100761, China

*E-mail: zhushaomin8888@sina.com.cn

Received February 13, 2009

A novel adaptive watermarking algorithm in discrete wavelet transform (DWT) based on quantization index modulation (QIM) technique is presented. The host image is decomposed into wavelet subbands, and then the approximation subband is divided into non-overlapping small embedding blocks. The secret watermark bit is embedded into singular value vector of each embedding block by applying QIM. To improve the invisibility and robustness of watermarking system, the quantization step for each embedding block is set by combining statistical model with particle swarm optimization (PSO) algorithm. The experimental results show that the proposed algorithm not only preserves the high perceptual quality, but also effectively stands against joint photographic experts group (JPEG) compression, low-pass filtering, noise addition, scaling, and cropping attacks, etc. The comparison analysis demonstrates that our scheme has better performance than the previously reported watermarking algorithms.

OCIS codes: 100.2000, 100.5010, 100.7410.

doi: 10.3788/COL20090707.0580.

With the rapid growth of multimedia and network technologies, digital media such as image, audio, video, and three-dimensional (3D) model are increasingly vulnerable to illegal copying and redistribution. Digital watermarking has emerged as a leading technique that is trying to solve problems related to copyright protection and content authentication of intellectual property of digital media. In short, digital watermarking refers to embedding a secret imperceptible signal (watermark) into host data. Two significant properties are often used to evaluate the performance of watermarking system. Firstly, the watermark should not affect the quality of host data. In other words, a watermarking algorithm is imperceptible if one cannot distinguish host data from that with the embedded watermark. Secondly, the embedded watermark should be robust and detectable after various intentional and unintentional attacks on host data. In authenticity applications, the watermark is required to be fragile. In this case, any changes to host data would damage the watermark[1,2].

In accordance with embedded position, watermarking can be divided into two categories: space domain and transform domain. The robustness of transform domain watermarking is better than that of the space domain watermarking generally[3,4]. Because discrete wavelet transform (DWT) has good time-frequency analysis characteristic and is consistent with human visual[5,6], the watermarking based on DWT has been one of the most important methods. Image matrix singular value decomposition (SVD) reflects the internal image characteristics and has good stability if image processing is performed. Therefore hybrid DWT-SVD watermarking schemes have been proposed recently. For example, Kim *et al.* proposed an approach emphasizing that watermark was embedded by modifying log-scaled singular values of selected coefficients of all subbands in DWT domain[7]. Ganic *et al.* described a hybrid DWT-SVD watermarking algorithm that after decomposing the host image into four bands and applying the SVD to each band, the same watermark data were embedded by modifying the singular values[8]. Bao *et al.* presented an adaptive DWT-SVD image watermarking that watermarking bit was embedded on the singular value of the blocks within wavelet subband of the host image, and modeled the adaptive quantization parameters based on the statistics of blocks within subbands[9]. However, most of these methods are non-adaptive or have not exploited the optimal features for more effectively embedding robust and secure watermark.

In this letter, we propose an optimal adaptive watermarking scheme based on hybrid DWT-SVD domain for gray scale images. The host image is transformed into wavelet subbands using DWT process. The approximation subband is segmented into small embedding blocks as the carrier of watermark information. Singular value vector of each embedding block is modified with quantization step to embed watermark. Because the quantization step is one of the key factors affecting the performances of quantization watermarking, the quantization step of each embedding block is optimally decided according to a statistical particle swarm optimization (PSO) method in order to reach a better trade-off between imperceptibility and robustness of digital watermarking system. Experimental results show that the proposed scheme not only has good visual quality irrespective of the nature of the chosen images but also is robust to image processing attacks.

PSO is a population-based stochastic optimization method introduced by Eberhart *et al.*[10]. In PSO, when a particle's neighborhood is defined as the whole swarm, the PSO is called the global version, otherwise it is called the local version[10]. In the following, the global version will be discussed.

In a D-dimensional space, the ith particle of the swarm can be represented as $X_i = (x_{i1}, x_{i2}, \cdots, x_{iD})$

and the velocity for the ith particle can be represented as $V_i = (v_{i1}, v_{i2}, \cdots, v_{iD})$. The best previous position of the ith particle is recorded and denoted as $P_i = (p_{i1}, p_{i2}, \cdots, p_{iD})$. The index of the best particle among all the particles in the swarm is represented as $P_g = (p_{g1}, p_{g2}, \cdots, p_{gD})$. During each iteration, each particle is updated with the velocity and location according to

$$V_{id}^{n+1} = \chi\Big[\omega v_{id}^n + c_1 r_1 (p_{id}^n - X_{id}^n) + c_2 r_2 (p_{gd}^n - X_{id}^n)\Big], \quad (1)$$

$$X_{id}^{n+1} = X_{id}^n + V_{id}^{n+1}, \quad (2)$$

where ω is the inertia weight value; $d = 1, 2, \cdots, D$, $i = 1, 2, \cdots, m$, and m is the number of particles in the swarm; X_{id}^n and V_{id}^n stand for the position and velocity of the ith particle of the nth iteration, respectively; r_1 and r_2 are random variables drawn from a uniform distribution in the range of [0,1]; c_1 is a cognitive acceleration constant and c_2 is a social acceleration constant; χ is the constriction factor.

Shi *et al.* have pointed out a significant improvement in performance of PSO method with a linear decreasing inertia weight (LDIW) strategy over the iterations[11]. During the early part of search, greater weight is adopted to make particles own more global search ability to explore new search areas, so as to determine the location of the optimal solution. On the other hand, during the latter part of search, when the algorithm is converging to the optimal solution, smaller weight is adopted to perform a better local search[11]. The mathematical representation of ω is

$$\omega = \omega_{\max} - \frac{\omega_{\max} - \omega_{\min}}{iter_{\max}} \times iter, \quad (3)$$

where $\omega_{\max}$ and $\omega_{\min}$ are the initial and final values of the inertia weight, respectively, $iter_{\max}$ is the maximum number of iterations, and $iter$ is the current number of iterations.

The embedding strength is more or less proportional to the perceptual sensitivity to distortions for using the quantization step. In order to resist the normal signal processing and other different attacks, we wish the quantization step as high as possible. However, because the watermark directly affects the host image, it is obvious that the higher the quantization step is, the lower the quality of the watermarked image will be. In other words, the robustness and the imperceptibility of the watermark are contradictory to each other. Based on the statistical model used in Ref. [9], we design the statistical-PSO model to further improve the robustness and transparency of watermark.

Supposing the host image is I that is decomposed in j levels DWT, we obtain the approximation subband LL_j and three detailed subbands HL_j, LH_j, and HH_j. We choose LL_j as the embedding region for its higher energy value and robustness against various attacks and processing. The scheme is detailedly described as follows.

Step 1: Segment LL_j into non-overlapping blocks A_i of size $k \times k$, $i = 1, 2, \cdots, M$, where M is the number of blocks.

Step 2: Calculate the average value m_{A_i} and standard deviation σ_{A_i} for each block A_i.

Step 3: Calculate the value δ_i for each block, which analyzes the homogeneity of each block according to

$$\delta_i = \delta_{\text{mean}} \times m_{A_i} + \delta_{\text{std}} \times \sigma_{A_i}, \quad (4)$$

where δ_{mean} and δ_{std} are the weighting parameters for m_{A_i} and σ_{A_i}, respectively, which are empirically set.

Step 4: Find the maximum value $\delta_{\max}$ and the minimum value $\delta_{\min}$ from all δ_i.

Step 5: Design the quantization step model for each block A_i as

$$d_i = d_{\min} + (d_{\max} - d_{\min}) \times \frac{\delta_i - \delta_{\min}}{\delta_{\max} - \delta_{\min}}, \quad (5)$$

where $d_{\min}$ and $d_{\max}$ are the minimum and maximum quantization step values, respectively, which are also randomly determined.

The choice of statistical model parameters such as δ_{mean}, δ_{std}, $d_{\min}$, and $d_{\max}$ in Eqs. (4) and (5) may be based on some general assumptions[9]. Here we utilize PSO to automatically determine these values without making any assumption and set proper quantization statistical-PSO model. In the application of PSO, we should consider four essential components as follows.

The first component is solution representation and initialization. The representation scheme determines how the problem is structured, as well as the iteration operators that can be used[12]. Each particle in the swarm represents a possible solution to the problem and hence consists of a set of model parameters for each block. Meanwhile, we randomly generate each particle value in the initial swarm. The second component is the fitness function. Because the structural similarity (SSIM) index analyzes the distorted image quality through comparing the correlations in luminance, contrast, and structure between the reference and distorted images, it is able to capture local dissimilarities better and has been shown to outperform mean square error (MSE) and the related peak signal-to-noise ratio (PSNR) in measuring the quality of natural images across a wide variety of distortions[13]. Therefore we consider that the SSIM index is the proper objective evaluation method for algorithm imperceptibility measurement. We use the following simple form of the SSIM index in our work:

$$\text{SSIM} = \left(\frac{2\mu_x\mu_y + C_1}{\mu_x^2 + \mu_y^2 + C_1}\right)\left(\frac{2\sigma_{xy} + C_2}{\sigma_x^2 + \sigma_y^2 + C_2}\right), \quad (6)$$

where x and y are two non-negative image signals to be compared; μ_x and μ_y are the mean intensity of x and y, respectively; σ_x and σ_y are the standard deviation of x and y, respectively; σ_{xy} is the covariance between x and y; the constants C_1 and C_2 are used to stabilize the metric for the case where the means and variances become very small to avoid the denominator being zero.

We utilize bit correct ratio (BCR) between original watermark and extracted watermark for representing algorithm robustness. In PSO optimization procedure, three common signal processing attacks are applied including Gaussian noise (GN), rescaling (RS), and Gaussian filtering (GF). Meanwhile, we can conveniently add or replace other attacking methods during PSO optimization process. BCR is defined as

$$\mathrm{BCR}(W', W) = \frac{\sum_{i=1}^{p}\sum_{j=1}^{q}\overline{w'(i,j)\oplus w(i,j)}}{p\times q}\times 100\%, \quad (7)$$

where $w(i,j)$ and $w'(i,j)$ represent the embedded and extracted watermarking bits, $p\times q$ denotes the length of the watermarking message, and $\oplus$ represents the exclusive-OR (XOR) operation. The watermarked image imperceptibility and robustness should be measured to formulate proper fitness function, which is defined as

$$f_i = -\left[\sum_{i=1}^{m}\mathrm{BCR}(W_i', W) + \mathrm{SSIM}(I_{\mathrm{W}}, I)\right], \quad (8)$$

where m represents the number of attacking methods, I_{W} is the watermarked image.

The third component is PSO optimization training. The similar PSO optimization training procedure proposed by Aslantas *et al.*[14] is adopted. A diagram of our PSO optimization training is shown in Fig. 1. The fourth component is the stopping condition. Once the number of training iterations in PSO is reached, the optimization process is stopped. The population with the smallest fitness value in the final iteration is the optimized quantization model.

The watermark image needs to be preprocessed in order to dispel the pixel space relationship and improve the robustness and security performance of the whole system. The extended Arnold scrambling is applied to the pretreatment of the binary watermark image[15]. We adopt the similar embedding procedure as that used in Ref. [9]. The embedding procedure can be described as follows.

Step 1: Compute the singular value vector of each block A_i by SVD,

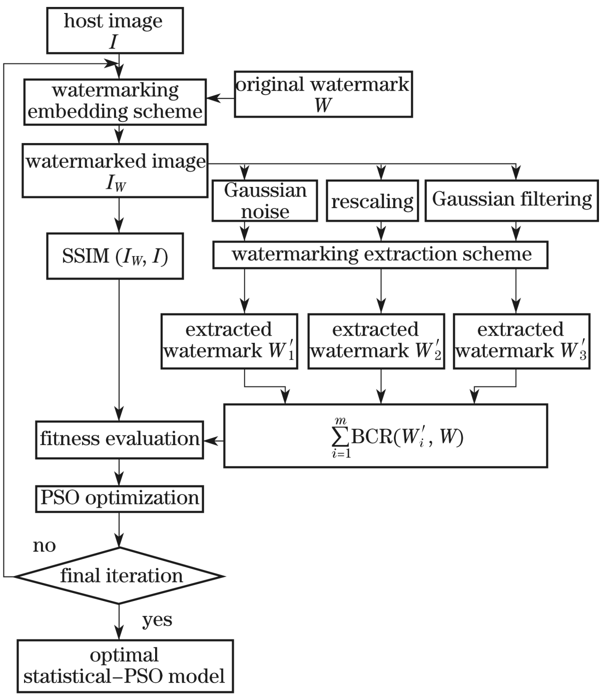

Fig. 1. Diagram of PSO training.

$$\mathrm{SVD}(A_i) = \boldsymbol{U}_i \sum{}_i \boldsymbol{V}_i^{\mathrm{T}}, \quad (9)$$

where $\boldsymbol{U}_i$ and $\boldsymbol{V}_i^{\mathrm{T}}$ are orthogonal matrices.

Step 2: Compute $N_{i\lambda} = \ \parallel \lambda_i \parallel +1$ and quantize it by optimal quantization step d_i^{opt} that represents the quantization level for correlating $N_{i\lambda}$ with A_i,

$$N_i = \left\lfloor N_{i\lambda}/d_i^{\mathrm{opt}}\right\rfloor, \quad (10)$$

where $\lambda_i = (\lambda_{i1}, \lambda_{i2}, \cdots, \lambda_{iw})$ denotes a vector formed by the singular values of each block A_i.

Step 3: Embed one watermark bit w_i by modifying the integer number N_i :

$$N_{iw} = \begin{cases} N_i + 1, & \begin{array}{l}\mathrm{mod}(N_i, 2) = 1 \text{ and } w_i = 1; \text{or} \\ \mathrm{mod}(N_i, 2) = 0 \text{ and } w_i = 0.\end{array} \\ N_i, & \text{otherwise} \end{cases} \quad (11)$$

Step 4: Compute the modified singular values by

$$(\lambda_{i1}', \lambda_{i2}', \cdots, \lambda_{iw}') = (\lambda_{i1}, \lambda_{i2}, \cdots, \lambda_{iw}) \times\left(\frac{N_{iw}\times d_i^{\mathrm{opt}}}{N_{i\lambda}} + \frac{d_i^{\mathrm{opt}}}{2N_{i\lambda}}\right). \quad (12)$$

Step 5: Compute the watermarked block A_i' with the modified singular values, reshape the watermarked approximation subband LL_j', and then obtain the watermarked image I_W using inverse discrete wavelet transform (IDWT).

The watermark extracting scheme is the inverse of the embedding procedure. Supposing that I_{W} is decomposed in j levels DWT, we obtain the approximation subband LL_j'. The extracting procedure is given as follows.

Step 1: Segment LL_j' into non-overlapping blocks A_i' of size $k\times k,, i = 1, 2, \cdots, M$, where M is the number of blocks.

Step 2: Compute the singular value vector of each block A_i' by SVD,

$$\mathrm{SVD}(A_i') = \boldsymbol{U}_i \sum{}_i{}' \boldsymbol{V}_i^{\mathrm{T}}. \quad (13)$$

Step 3: Compute $N_{i\lambda}' = \|\lambda_i'\| + 1$ and quantize it by optimal quantization step d_i^{opt} :

$$N_i' = \left\lfloor N_{i\lambda}'/d_i^{\mathrm{opt}}\right\rfloor, \quad (14)$$

where $\lambda_i' = (\lambda_{i1}', \lambda_{i2}', \cdots, \lambda_{iw}')$ denotes a vector formed by the singular values of the block A_i'.

Step 4: Extract watermark bits according to

$$w_i' = \begin{cases} 1, & \text{if} \quad \mathrm{mod}(N_i', 2) = 0 \\ 0, & \text{if} \quad \mathrm{mod}(N_i', 2) = 1 \end{cases}. \quad (15)$$

Step 5: Reshape the original binary watermark image by performing inverse extended Arnold scrambling on watermark image.

The performance of the proposed algorithm was tested on a large number of experiments. Here the results are presented for gray scale 8-bit Lena, Peppers, and Baboon images of size 512×512 with different textures, as depicted in Fig. 2. The logo used for watermark image is the binary image of size 64×64 as depicted in

Fig. 3. For one-level wavelet decomposition, Haar filter coefficients are used, and k is generally set to 4. Table 1 summarizes the fundamental values for optimization process in the proposed scheme. At the same time, the experiments compared the performances of the proposed algorithm with Bao's algorithm[9], which is a DWT-SVD watermarking based on adaptive quantization step.

Figures 2(a)−(c) show the host images and Figs. 2(e)−(f) show the watermarked images. Subjectively, it seems difficult to distinguish the difference between the host and the watermarked images by the human eyes. Objectively, PSNR is used efficiently to measure the visual fidelity between the host and watermarked images. It is found that the image qualities measured by

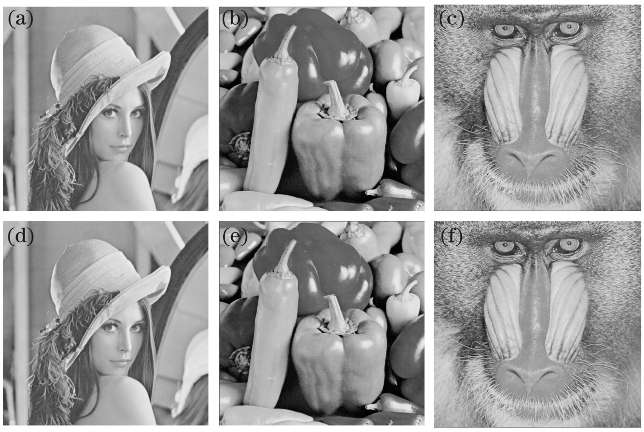

Fig. 2. Host and watermarked images. (a) Lena; (b) Peppers; (c) Baboon; (d) marked Lena; (e) marked Peppers; (f) marked Baboon.

Fig. 3. Orignal watermark image (left) and scrambled image (right).

Table 1. PSO Fundamental Parameters

Parameter	Value
Swarm Size	40
Particle Dimension	4
Velocity Weight at the Beginning	0.95
Velocity Weight at the End	0.40
Cognitive Acceleration	2
Social Acceleration	2
Iterations	200
Constriction Factor	1

Table 2. Values of PSNR (dB)

Image	Proposed Scheme	Bao' Scheme
Lena	40.8128	39.3839
Peppers	40.5337	38.9264
Baboon	40.1752	37.4773

Table 3. Experimental Results after Different Attacks

Attack	Attacked Image	Extracted Watermark	NC	BER (%)
No Attack		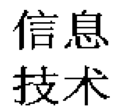	1.0000	0.0000
Gaussian Noise (var 0.1%)			0.9027	14.7705
Pep&Salt Noise (density 0.5%)			0.8846	17.3096
Gaussian Filtering		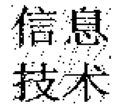	0.9742	4.0283
Median Filtering		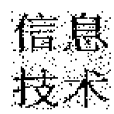	0.9559	6.8115
Scaling 25%			0.9048	14.4043
Cropping 25%			0.9173	12.5977

PSNR among the watermarked images are all greater than 35 dB. This indicates that the proposed watermarking scheme has good visual fidelity. Meanwhile, Table 2 simultaneously compares in terms of PSNR for evaluating the visual fidelity performance of our scheme with Bao's scheme.

The watermarking scheme should be robust to common signal processing which could be intentional or unintentional. Normalized correlation (NC) and bit error ratio (BER) are adopted for evaluating the robustness of the watermarking scheme. Without any image attack, the NC value is 1 and the BER value is 0. In other words, the watermark can be completely extracted. Table 3 illustrates the results after various attack operations on the watermarked Lena image including noise addition, low pass filtering, scaling, and cropping.

Finally, we test the robustness by JPEG compression which is one of the most important attacks with different quality factors (QFs). The results are shown in Table 4 for the BER versus JPEG compression. Compared with Bao's scheme, it is observed that there is a higher robustness to JPEG compression with the proposed scheme.

In conclusion, we propose a novel quantization index modulation watermarking algorithm in hybrid DWT-SVD domain. After decomposing the host image by

Table 4. Comparison of Experimental Results under JPEG Compression

QF	Proposed Scheme's BER(%)				Bao's Scheme BER(%)			
	Lena	Peppers	Baboon	Average	Lena	Peppers	Baboon	Average
70	0.0000	0.0000	0.0000	0.0000	0.0000	0.0000	0.0000	0.0000
60	0.0000	0.0977	0.0244	0.0407	0.9600	0.6400	0.0000	0.5333
50	0.0244	0.1465	0.1465	0.1058	3.0400	1.4400	0.4800	1.6533
40	1.8799	1.6113	0.7813	1.4242	8.3200	5.7600	1.6000	5.2267

DWT, watermark information bit is embedded into the singular value vector of each embedded block within approximation subband of the host image. A novel quantization step model is a design based on statistical feature and PSO. The experimental results show that the proposed scheme not only preserves the high perceptual quality, but also is robust against many types of attacks.

References

1. G. Langelaar, I. Setyawan, and R. L. Lagendijk, IEEE Signal Processing Mag. **17,** (5) 20 (2000).
2. Y. Hu and S. Zhu, Acta Opt. Sin. (in Chinese) **28,** 1691 (2008).
3. L. Zhang, W. Xiao, G. Qian, and Z. Ji, Chin. Opt. Lett. **5,** 21 (2007).
4. L. Li, B. Guo, and K. Shao, Chin. Opt. Lett. **5,** 332 (2007).
5. Z. Li, F. Xia, G. Zheng, and J. Zhang, Chin. Opt. Lett. **6,** 251 (2008).
6. Y. Wang, T. Liu, and J. Jiang, Chin. Opt. Lett. **6,** 657 (2008).
7. K.-S. Kim, M.-J. Lee, and H.-K. Lee, in *Proceedings of the Third International Conference on Intelligent Information Hiding and Multimedia Signal Processing* 477 (2007).
8. E. Ganic and A. M. Eskicioglu, in *Proceedings of the 2004 Workshop on Multimedia and Security* 166 (2004).
9. P. Bao and X. Ma, IEEE Trans. Circ. Syst. Video Technol. **15,** 96 (2005).
10. R. Eberhart and J. Kennedy, in *Proceedings of the Sixth International Symposium on Micro Machine and Human Science* 39 (1995).
11. Y. Shi and R. C. Eberhart, in *Proceedings of IEEE International Conference on Evolutionary Computation* 1945 (1999).
12. C.-C. Lai, H.-C. Huang, and C.-C. Tsai, in *Proceedings of 2008 International Conference on Intelligent Information Hiding and Multimedia Signal Processing* 469 (2008).
13. Z. Wang, A. C. Bovik, H. R. Sheikh, and E. P. Simoncelli, IEEE Trans. Signal Processing **13,** 600 (2004).
14. V. Aslantas, A. L. Doğăn, and S. Ozturk, in *Proceedings of 2008 IEEE International Conference on Multimedia and Expo* 241 (2008).
15. S. Zhu and J. Liu, in *Proceedings of 2008 International Symposium on Knowledge Acquisition and Modeling* 668 (2008).